Computer Fraud and Security
ISSN (online): 1873-7056

Test-Driven Design for AI-Focused Hardware Platforms

Karan Lulla
Senior Board Test Engineer, NVIDIA, SantaClara, CA, USA
karanvijaylulla08@gmail.com
Orcid: 0009-0007-7491-4138

Article Received: 12 March, 2024 **Accepted:** 21 May, 2024 **Published:** 18 June, 2024

Abstract

The paper explores how competitive, technology-agnostic AI-centered hardware can integrate test-driven design (TDD) both within and outside of the system. The method requires writing executable tests before implementation, binding oracles that involve the golden model on the boundary with tensors, operators, and kernels, and continuously integrating and automating regression testing of the simulation, emulation, and prototype targets. Multi-tier stimuli (unit, integration, system) are operationalized, acceptance envelopes created around possible numerical correctness (e.g., 0.5 percentage-point top-1 delta vs. FP32 with INT8/FP16), and the correctness performance and energy gates are linked. Empirically, it has been found that the method can raise pre-tape-out functional coverage to ≥95% (measured at 97.1%), code/toggle coverage to ≥90%, and mean time-to-repair by a factor of ~40% (10.1→6.0 days). In representative workloads (ResNet-50, MobileNet-V3, Transformer, and streaming ASR), the p99 latency is reduced by ~11–13%, throughput is increased by ≥10%, and power usage is decreased by ≥12% (inferences/J) with no notable differences in accuracy. Fault injection and environmental corners are used to increase reliability, and fleet-style telemetry can detect and roll back early issues. Benchmarking is based on MLPerf-style KPIs, and both tails and medians are reported. Additionally, regression bisection is automatically performed to distinguish between compiler and RTL causes. The findings indicate that hardware-centric TDD offers a feasible, supply-side blueprint that reduces the re-spin risk (approximately 15%) and speeds up the time-to-market, with artifacts that are reproducible across data centre and edge deployments. Artifacts and datasets are published to facilitate replication studies.

Keywords; Test-Driven Design (TDD), AI hardware verification & validation, Hardware–software co-design, Quantization drift (INT8/FP16), MLPerf-style benchmarking.

1. Introduction

AI performance parameters have grown by millions, then expanded to trillions of parameters, multiplying the need for leading-edge compute resources. The cost of training a state-of-the-art transformer can surpass 1e23 floating point calculations and run for weeks on its thousands of accelerators. In the meantime, interactive search, vision, and speech competitive inference aim for a 95th percentile (p95) latency of less than 10 ms with a controlled 99th percentile (p99). The demands conflict with the enduring hardware constraints: limited on-chip memory in the form of SRAM compared to working sets; limited off-chip bandwidth, even with multi-accelerator schedules, using HBM3e; and contention at the interconnects of multi-accelerator schedules. Frequency and voltage scaling are hindered by constraints in thermal and power envelopes, which increases the incentive to scale based on numerically efficient kernels and ensures that no microarchitectural changes are made.

The traditional techniques of network-on-chip and system-on-chip development often delay complete verification until late integration, when the error is most expensive to fix. A single bug during the layout at advanced nodes may result in a re-spin of $10 -20 million and a schedule slippage of 8-12 weeks. In the case of AI accelerators, there are other failure modes due to opaque numerics, such as quantization, stochastic rounding, kernel fusion, and sparsity, which can cause accuracy errors that may go unnoticed by naive unit tests. Annually, parallel execution becomes nondeterministic by the law of race or timing. Software levels, such as compilers and execution environments, develop autonomously. This can introduce hardware/software drift, which invalidates previous results unless they are constantly validated. The discovery of defects should again shift to the left, utilizing quantifiable gates that prevent regressions, minimize numerical drift, and ensure that performance budgets align with real-world expectations.

This paper assesses the concept of test-driven design (TDD) adapted for AI-oriented hardware systems, including RTL, FPGA prototyping, and ASIC designs. It defines executable tests before implementation, documents golden-model oracles along with RTL, kernel boundaries, and permits integration by automatic regression involving RTL, firmware, and compiler passages. Measures taken are quantified into such targets as: at least 95% of operational functions and code coverage before tape-out, deltas in bound accuracy of ≤ 0.5 percentage points between FP32 benchmarks and INT8/FP16

quantization, system improvements: of ≥ 15% median latency improvement, ≥ 10% throughput improvement, ≥ 12% improvement in energy consumption measured as inferences per joule on representative workloads.

It encompasses the scope of GPUs, non-processing units, and FPGAs that are used in data centers, as well as edge environments. The representative workloads include ResNet-50 and MobileNet-V3 (vision), GNMT-type LSTMs and BERT-base encoders (language), as well as mixed-precision training and inference flows. Utilizing Verilog/SystemVerilog RRL, UVM constrained-random testbenches, SystemC/TLM co-simulation, and Python or C++ code reference harnesses to create golden models, which are used as benchmarks. The thermal behavior and power are determined based on emulation-generated traces and activity estimates done at the gate level. It has limitations, such as omitting analog in-memory computing and wafer-scale computing, and is practically limited in the size of datasets and the availability of devices. It analyzes the stochastic operation of seed control to evaluate stochastic operators and recreates the deterministic execution of traces to identify the location of Heisenbugs. The use of modeling thermal derating and voltage droop is also examined to verify guardbands.

This research is structured into different chapters. Chapter 2 summarizes the existing literature on TDD concepts, hardware verification, and trends in AI architecture, motivating a measurement-focused approach. Chapter 3 presents several methods, including test taxonomy, oracle design, continuous integration pipelines, and acceptance thresholds for coverage, accuracy, latency, and energy efficiency. Chapter 4 provides an explanation of AI-specific verification and validation, including quantization-drift limits, fault-injection and stress reliability, and standardized benchmarking based on MLPerf-style KPIs. Chapter 5 documents experimental configurations and findings on FPGA prototypes and emulation systems, providing statistics and confidence intervals. Chapters 6-8 cover implications, outline future work, and give a conclusion, offering practical advice to platform teams with traceable metrics mapped to service-level goals and a verifiable artifact bundle.

2. Literature Review

2.1 Evolution of TDD

Test-driven development (TDD) was invented in the field of software engineering, where tests are executable and both the implementation and the test execution are performed line by line, with small and verifiable increments, providing instant feedback. There are no precedents in single-process software for concurrency, timing, and observability restrictions that single-process software does not have, when expressed in either embedded or hardware description language (HDL). Hardware modules also connect through protocols, resets, and clocks, and verification therefore has to coordinate the stimulus, monitors, and checkers across a myriad of interfaces in parallel. Orchestration of the event [30]. The testbenches are required to respond to transactions, interrupts, backpressure, and timeouts in a manner that is deterministic enough to facilitate debugging of the test.

As shown in the figure below, the TDD loop operates as follows: write a test, observe it fail (red), write the smallest amount of code necessary to make it pass (green), refactor, and iterate, providing executable line-by-line feedback. This cycle, in hardware and embedded contexts, must deal with concurrency and timing: not only with protocols, resets, and clocks between modules, but also with verification, coordinating stimuli, monitors, and checkers across a myriad of interfaces. Testbench Deterministic testbenches control transactions, interrupts, backpressure, and timeouts to facilitate failures that repeat exactly, enabling fine-grained debugging and maintaining software TDD discipline in HDL verification on a production scale.

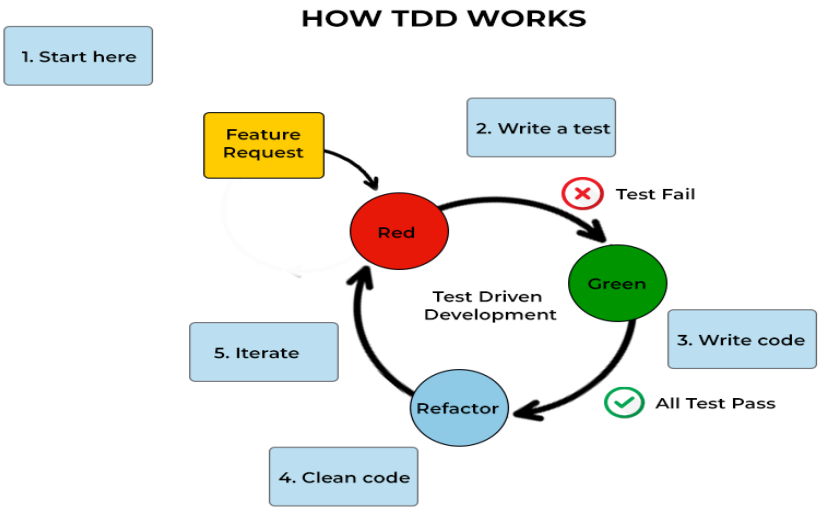

Figure 1: TDD cycle: deterministic tests guiding concurrent hardware verification

The conceptual template provided by the architectural underpinnings of event-driven microservices, namely producers, consumers, topics/queues, idempotency, and at-least-at-most-once delivery semantics, is used to conceptualize the organization of a verification environment that should withstand ordering variability and partial failures. In hardware verification, this corresponds to scorecards, drivers, and sequencers that are connected via events and assertions, along with test fixtures, to test the injection of faults and recovery. Explicit interface contracts and quantifiable acceptance criteria (e.g., latency budgets, protocol coverage) are promoted by first designing tests, which is also consistent with pipeline decomposition at the register-transfer level (RTL) blocks. However, there are challenges to adaptation: one cannot easily observe what takes place inside the synthesis; there is nondeterminism due to arbitration; and timing closure can render prior assumptions invalid due to microarchitectural changes, pressurizing event-aware test harnesses and decoupled oracles [4].

2.2 AI Hardware Trends

General-purpose GPUs, domain-specific tensor/AI processors (TPUs/NPUs), and reconfigurable FPGAs have all been implemented in AI hardware. Precision modes defined across these targets determine the arithmetic units, memory footprints, and data flow. FP32 serves as an accuracy reference, FP16/BF16 are used to accelerate training, and FP8 or lower are utilized for high-density inference. Mixed-precision scheduling makes verification as challenging as having an upward selection of precision by different layers or operators, and retaining higher precision in accumulators to prevent devastating cancellation [12]. Practical usage is limited by memory bandwidth, on-chip buffer sizes, and the use of operator fusion and tiling techniques, which differ between platforms. Additionally, duty generates hardware surfaces of software interactions that must be regression-tested each time either a compiler or a kernel is modified.

Workloads are also shifting from unimodal image recognition to multimodal pipelines, where text, vision, audio, and sensor streams are integrated, and thereby augmenting heterogeneity within tensors, sequence lengths, and temporal coordinates. Multimodality emphasizes pre- and post-storage and processing, as well as cross-domain synchronization. It sets high standards for test oracles that must confirm end-to-end semantics, rather than relying on single-operator numeric. These attributes drive a literature perspective where verification is not only arithmetically accurate but also data flow well-formed and includes read-only invariants, desirable for the pragmatic requirements of models processing language, images, and signals collectively [31].

2.3 Traditional vs. Test-Driven Hardware Design

Conventional hardware streaming focuses on specification and design, block testing, as well as high-level verification, and end-to-end bring-up, which is typically only done when prototypes or first silicon are available. On the occasions that this sequencing presents defects, such as protocol mismatches, reset races, clock-domain crossings, or throughput shortages, changes are most costly [3]. The growth of coverage is back-loaded; change management directly creates artifacts of verification closely tied to implementations, which can be easily refactored. By contrast, a test-based method indicates that realizable contracts precede the existence of RTL latency cocoons and precision conveniences, which comprise interface claims, latency capsules, and accuracy margins, as evidenced by red tests that direct minimal implementation to green. At the unit level, stubs serve as a means of anchoring stimulus and oracles early on, allowing for continuous integration and coverage, as well as defect density and performance proxies (cycles per inference on emulation) to be measured.

Since expectancies are coded independently of microarchitecture expectancy, designers can investigate how much pipeline depth, buffering, or scheduling can be explored without causing invalid reactions to system behavior, and compilers can evolve kernel fusion while remaining within their accuracy deltas. Publish/subscribe stimulus, retry logic, and dead-letter scores are event-focused design patterns in software, which are converted into transaction scoreboards, response timeouts, and quarantine paths to enhance verification, reordering, and back pressure resistance. The overall impact is that it causes a shift to earlier bug discovery, higher coverage monotonicity, and less integration predation (constrained behavior) by continuously running, version-controlled tests.

2.4 Prior Studies & Metrics

Empirical reporting on TDD-related practices in AI systems research often focuses on model-level validation, rather than hardware, and encompasses a variety of strands inspired by measurable verification objectives. The study of dynamic memory and attention processes in natural language inference places special emphasis on sensitivity to sequence structure, gating, and selective retrieval [9]. It is not just numerically equal, but it also maintains relational and temporal links among steps. To handle hardware verification, this suggests test oracles that monitor invariants of memory access patterns, pointer lifetimes, and control-flow decisions, but not scalar outputs.

Generalizing metrics include sequence-level accuracy windows, limited divergence under precision modification with a golden model, and covering state transitions that involve memory reads/writes. These views promote adversarial models as inputs to the verification harnesses that produce adversarial and long-range dependency inputs, and hold properties that assert about intermediate representations, rather than only final logits. They propose, as well, to measure bug-finding yield as itself a function of input curriculum complexity (such as in terms of length of sequence or depth of

memory to reveal corner cases in cache/coherency or tensor gather/scatter units). To make TDD artifacts predictive of reliability in field affordance under language or reasoning loads [26].

2.5 Gaps in Current Research

There are numerous areas of gaps within the surveyed literature where TDD and AI-oriented hardware co-exist. Machine-learning numeric taxonomies are in a primitive state. No widely agreed-upon schema exists to categorize tests by operator type, precision regime, and tolerable accuracy deltas between compilers and hardware, despite the apparent requirements of mixed-precision and quantization approaches. The cross-platform reproducibility is also low, as the same model is frequently compiled to a different backend, differing in kernel schedules, fusion, and memory layouts [34]. However, the area lacks event-aware fixtures that would ensure timing and ordering tolerances are maintained and semantic equivalence is preserved.

Benchmarking is more likely to highlight aggregate measures of quality and understate the existence of latency distributions, tail behavior, and power-normalized throughput in the face of realistic pre- and post-processing metrics that are needed to induce the use of regression gating (regression), as well as meaningful service-level targets. Very little research also describes change-management practices that anchor tests to specifications, as opposed to implementations, which necessarily reduce the reuse of verification assets between different microarchitectural refactors. Microservices, Event-driven progress, though succinctly described, still lacks a significant history of systematic translation into hardware test infrastructures, such as the idempotency of side effects, exact once delivery counterparts to DMA transactions, and compensating actions when a part of the system fails. These gaps fill the verification mismatch between the heterogeneity and the magnitude of modern AI applications, allowing the application of statistically reasonable acceptance criteria and enabling TDD to serve as a unifying mechanism across compilers, runtimes, and silicon platforms.

3. Methods and Techniques

3.1 Test-Driven Design Workflow for Hardware

This design philosophy is a software implementation of the test-driven design (TDD) concept, ensuring that AI-oriented hardware has its executable tests written in advance, before any register-transfer level (RTL) or high-level synthesis source code is generated. Each feature contains an initial failing test, an interface contracts specification, a timing specification, and numerical tolerances. Implemented as golden models, in Python or C++, which generate canonical outputs at the bottom of tensors, operators, and kernels, and acceptance envelopes are static [29]. In the case of vision and language workloads, the harness guarantees that for tension achieves top-1 accuracy deviation of less than 0.5 percentage points before quantization equivalence and transient error of less than 1% with respect to tensor metrics, all within fixed, tailored acceptance envelopes. Tests are arranged at the unit, integration, and system levels and assigned non-editable requirement IDs to provide their traceability.

As presented in Figure 2 below, acceptance TDD and developer TDD will run concurrently, writing an acceptance test, running that acceptance test, and repeating with small tests as developer tests implement fine-grained behavior. Language checks for RTL/HLS are pretested in executable tests that enforce interface contracts, timing constraints, and numeric tolerances using Python/C++ golden models. The reason why failing tests lead to minimal changes is that the developer and acceptance suites are not working correctly. Tests with unchangeable requirement identifiers, arranged into unit, integration, and system levels, maintain traceability and acceptance envelopes of the tests.

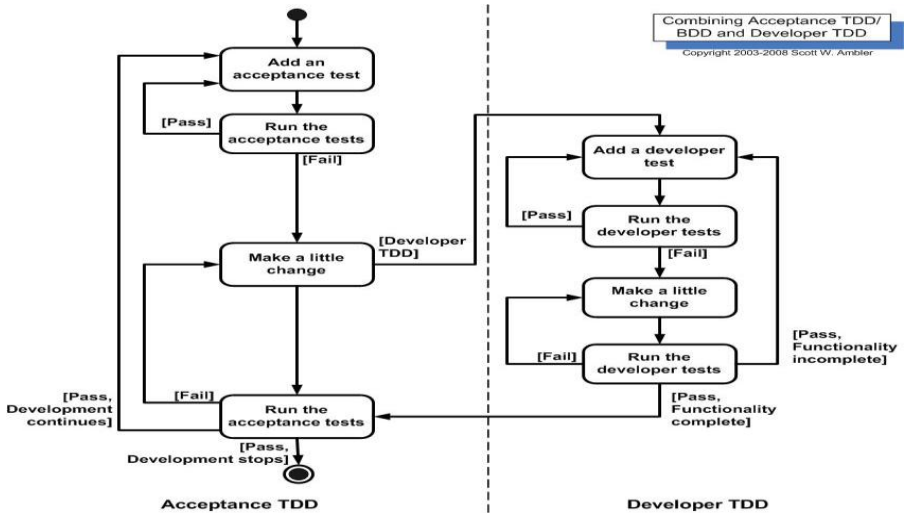

Figure 2: Combined acceptance/developer TDD loops for pre-RTL, test-first workflows

Three layers of stimulus are produced. Unit stimulus exercise leaf modules, such as a multiply-accumulate array, DMA engine, tensor interleaver, and cache tiles, are exercised using constrained-random strides, dilations, and densities. The sparsity density varies between 0% and 90%, and burst sizes range from 4 to 16 states-of-the-art KB. Near-arbitration starvation and credit underflow are triggered by integrating stimuli with on-chip networks and memory hierarchies, which involve 8-32 outstanding reads, hot/cold address mixes, and injected backpressure, accounting for 10-40% of the total pressure. End-to-end models, including ResNet-50, MobileNet-V3, BERT-base, and streaming ASR, are replayed at boosted deployment-realistic batch sizes, challenging compiler fusion decisions as well as runtime scheduling with golden oracles.

Ecoflow Runner Automated regressions will operate using the simulator and emulator pools. Nightly suites are larger, with 10,000 or more test cases to run, with a wall-clock cost of 10 or 12 hours; per-commit smoke suites run in 20 minutes or less. Failure on failures causes scripts to have a run-to-emission of waveform bookmark triage, minimized random seeds, logic cone reductions, and counterexample traces. The flake-rate ceiling is 1%, and all tests that have passed the threshold are in quarantine and being repaired [27]. The mean time to triage is set at 30 minutes for smoke failures and less than 4 hours for nightly regressions. Pre-tape-out criteria include 95% functional coverage, 90% code coverage, and zero open P0/P1 defects.

3.2 Verification and Validation Techniques

Formal verification is a means of providing exhaustive proofs of localized properties, which are seldom achieved through simulation. SystemVerilog Assertions, including safety properties APIs such as no write without grant on AXI bridges, no underflow/overflow in FIFOs, no stale credit in flow control, and no lost wakeup in interrupt controllers, are discharged through bounded model checking. With fairness constraints, liveness obligations are approximated, using progress counters [21]. Data path block proof-depth goals of 64 -128 cycles and control pipeline proof-depth goals of 256-512 cycles find a trade-off between capacity and payoff. Simulation coverage, combined with proof cores and bounded-depth coverage, completes the gaps.

Table 1: Summary of verification & validation techniques and acceptance targets

Technique	What it validates	Key configuration/targets	Acceptance/output
Formal verification (SVA + BMC)	Local safety/liveness properties	AXI grant, FIFO under/overflow, credits, interrupts; proof-depth: 64–128 cycles (datapath), 256–512 (control)	Proofs discharged; merge proof cores with simulation coverage
Constrained-random simulation (UVM)	Breadth across shapes/precisions/schedules	INT8/FP16/BF16; tiling/fusion sweeps; cross-coverage (e.g., INT8 accumulate in BF16; batch=1, seq=2048)	Coverage gaps identified; reproducible failing seeds generated
Statistical validation	Defect reproducibility & stability	≥30 failing seeds to declare defect; post-fix escape rate <1/1000 runs; p95/p99 from ≥1,000 iters (95% CI)	Closure only when thresholds met; latency/throughput budgets respected
Co-emulation / acceleration	Long-run, system-scale behavior	Timing-annotated netlists on ZeBu/Palladium; 10^3–10^5× faster than RTL	Supports ≥10k nightly tests and 24–48h soak runs
Field I/O replay	Protocol adherence under realistic ingress	Replayed PCIe/Ethernet, camera, audio captures	End-to-end quality validated; rare faults surfaced
Power & thermal checks	Energy efficiency and limits	Activity-based estimation + board sensors	≥10% inferences/J vs. prior RTL without thermal violations

Randomization and constrained-random simulation provide breadth-simulation. The UVM environment is optimized for tensor shapes, precision regimes (INT8, FP16, BF16), tiling, and fusion options for the compiler. Interactions of the form (INT8 accumulate in BF16), (batch=1, sequence length=2048) are being monitored in cross-coverage bins to make sure long-tail cases are being executed. The statistical stopping rule requires 30 or more independent failed seeds to

declare an observable defect and requires a post-fix escaping rate of less than 1 in 1000 runs to claim closure. Online enforcement accuracy windows are monitored through streaming Oracle and are often bounded by p95 and p99 with 95% certainty across 1000 or more iterations per configuration to sample latency and throughput.

The speed gap between system-scale testing and single-unit testing is overcome by co-emulation and acceleration. Timing-annotated netlists can be simulated as Timing-annotated hardware emulators (e.g., Synopsys ZeBu, Cadence Palladium), showing speedups of 10^3–10 ^5 times over RTL simulation of long sequences. This throughput supports nightly tests of 10k and above, as well as weekly 24-48 hour soak tests, which reveal memory leaks, deadlocks, and infrequent livelocks. Emulator farms are similar to field I/O: PCIe and Ethernet traffic, camera frames, and audio streams are replayed based on captures, ensuring that protocol compliance is followed and that there is end-to-end quality in the presence of realistic ingress. Power and thermal traces are gathered using activity-based estimation. The acceptance criteria are 10% or greater energy-efficiency features (inferences/J) compared to the previous RTL base, which does not violate thermal limits at the board level.

3.3 Hardware-Software Co-Design

Since compiler graphs and runtime schedulers play significant roles in hardware, co-design is an essential component. SystemC/TLM models serve as RTL twins at the transaction level, allowing driver bring-up and integration with the kernel to be done months before systems become usable with RTL. Shared with a standard library are typical instantiations of the same datasets, quantization tables, random seeds, and tolerances, which are used with SystemC, RTL simulation, emulation, and FPGA prototypes, thereby eliminating skew. Model-parity tests compare intermediate tensors between layers; an error of more than 1% relative or an accuracy difference of less than 0.5 percentage points between models would cause the build to fail [13]. The compiler passes emit manifests of fairness in the form of tile sizes, fusion boundaries, and memory layouts, which are understood as test inputs to provide a continuum of test exercises for schedule changes.

Rocket cores are connected to a RoCC matrix-multiply accessor via the TileLink system, memory, periphery, and control buses, satisfying hardware-software co-design, as shown in Figure 3 below. SystemC/TLM twins enable the very early bring-up of drivers as shared datasets and quantization tables, seeds, and tolerances, maintaining parity between RTL, emulation, and FPGA. Model-parity tests gate merge in the case of a difference between the layer tensors of >1% or a change in end accuracy of more than 0.5 pp. Compiler outputs include tile sizes, fusion breakdowns, and memory layouts, which are fed into continuous check exercises and validation.

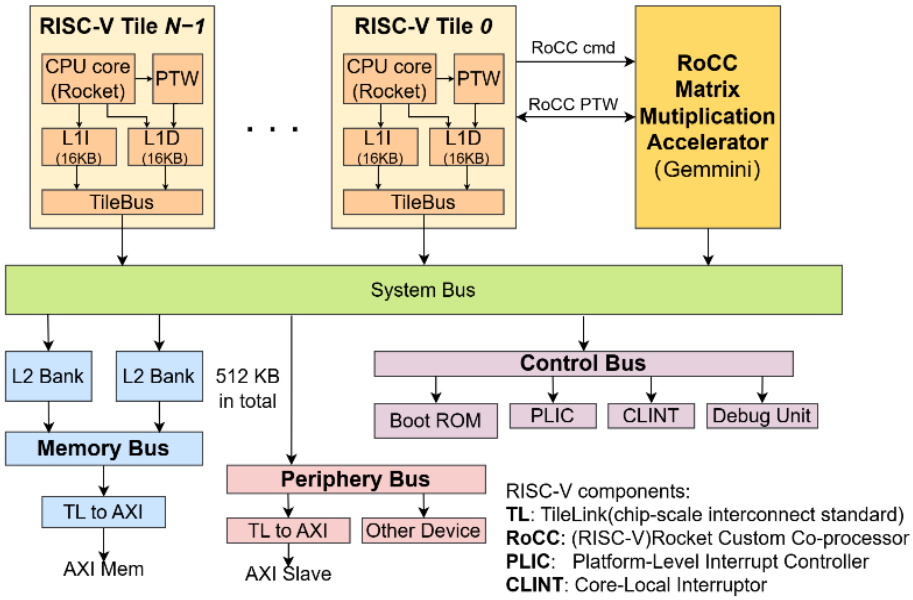

Figure 3: RISC-V SoC with RoCC accelerator and tile-linked co-design buses

The approach enables a 20% reduction in integration time compared to sequential flows, which involve staging hardware and software separately. This estimate is based on cycle-time instrumentation, specifically parity tests performed during each compiler commit and each merge step in the RTL, which reduces the average time to detect incompatibilities from days to hours. A service-level goal is to have 4 hours of handout time, adjusting for judgment of consistency, with suites exceeding three canonical models per area (view, vocabulary, sound) [14]. To handle nondeterminism, the harness can assist with deterministic replay through seed pinning and traffic capture/replay, and it logs sufficient metadata about tool versions, commits, manifests, and seeds to recreate any failure within a day.

3.4 Continuous Integration in Hardware Design

There is continuous integration (CI), which coordinates linting, synthesis, simulation, emulation, and packaging, with release gates having metrics that can be measured. That pipeline includes RTL, constraints, and testbench code static analysis and style checks; path sanity fast synthesis and static timing; unit and integration simulations and coverage harvesting; emulation submission and artifact collation; packing of bitstreams, compilers, and firmware into reproducible units. Gates have 95% or more functional coverage, a test flake rate of 1% or less, a p95 latency of model-specific budget constraints, and ≥ 12% energy efficiency relative to the previous baseline [8].

Table 2: An overview of CI stages, gates, and KPIs for hardware design

CI stage / activity	Metrics / gates	Outputs / KPIs
Lint, style, BoM scans (RTL, constraints, testbench; third-party IP/plugins)	Static checks clean; supply-chain hygiene verified	Secure, traceable sources; issues auto-blocked
Fast synth & static timing (path sanity)	No gross violations; clocks/resets sane	Early timing feedback; reduced late surprises
Unit & integration simulation with coverage harvest	≥95% functional, ≥90% code/toggle; flake rate ≤1%	Merge eligibility; unified coverage dashboard
Emulation submission & artifact collation	Queue SLA met; reproducible seeds/manifests captured	Deterministic replay; long-run validation enabled
Packaging (bitstreams, compilers, firmware)	Reproducible bundles built per commit	Auditable releases; environment parity
Performance gates	p95 latency within model budget; ≥12% energy efficiency vs prior baseline	Performance/energy regressions prevented
Stability gates	Repro success ≥99%; test flakes quarantined	Reliable CI signal; low noise
Operational KPIs	Defects/1000 LOC; MTTR <2 days (P1); ≥5 green mainline builds/day	Throughput and quality tracked continuously

Those operational KPIs are the defects/1000 LOC, the mean time to repair (goal of < 2 days on P1), and build made (≥5 green mainline builds/day). Analogy CI integrates security and supply-chain hygiene, with static and dynamic application security testing corresponding to lint and simulation and emulation behavior, respectively. Software composition analysis scans are visible as bill-of-materials scans of third-party IP, verification IP, and tool plug-ins [16].

4. Hardware Verification and Validation for AI Systems

4.1 Verification Challenges in AI Chips

This is because verification of AI accelerators should struggle with non-determinism, which in turn requires bit-exact testing. Reductions of atomic reorder partially-summed values, cache reorder random accesses, network-on-chip reorder random values, and asynchronous DMA propagate arrival jitter. As such, statistical envelopes are characterized by, and not equal to, verification. The conditions to be satisfied involve a 100th-percentile top-1 difference with an FP32 golden model following quantization, a percent error in the mean value of the middle tensors, and a KL-divergence in output probability values of 10^-3. The application of quantization drift also complicates oracles [23]. INT8 pipelines may physically reduce activations and leave higher-precision accumulators unchanged, resulting in asymmetric tolerances per layer. In kernel fusion, the accumulation order, associativity, and tiling boundaries may change; therefore, tests must assert that the results of invariants remain the same when schedules are changed.

Precision loss is also observed in corner cases, such as denormals and saturations, as well as mixed-precision accumulators. Unit tests must verify input ranges, sparsity, 0-90% sparsity, and stride and dilation grids. To limit non-determinism, it utilizes pin seeds, logs traffic for deterministic replay, and compares the layer-wise outputs with tolerances that progressively decrease as tensors are transformed into logits. The performance mindful checks run concurrently to ensure correctness: p95 and p99 latency should not exceed model-specific budget constraints, and throughput and energy expectations need to be met. Coverage should also be multi-facet: Before tape-out, functional coverage must be 95%, and

at control, toggle/branch coverage must be 90%, cross-coverage across (precision regime), (batch size), (sequence length), (fusion level).

4.2 Fault Tolerance and Reliability Testing

Reliability is ensured by fault injection and environmental testing, which reflect real-world deployment conditions. Soft-error Changing single bits in the register files, accumulator trees, SRAM arrays, and interconnect FIFOs in response to Poisson processes scaled to upset rates; silent data corruption (SDC) is established independent of the detected-and-corrected (DUE) counterparts. Goals are SDC < 1 per 10 12 operations with representative traffic and no escalation, which goes to system resets. As highlighted in Table 3 below, watchdogs need to identify 99.9% or more of control-path hangs within 10 ms, and recovery remedies— checkpoint/rollback, selective re-compute, and operator-level replay—must also fall within the service p95.

Table 3: An overview of fault-tolerance and reliability test strategy

Aspect	What it tests	Configuration / Stressors	Pass / Target Metrics
Soft-error injection	Sensitivity to transient bit flips	Flip single bits in RFs, accumulators, SRAMs, NoC FIFOs using Poisson processes scaled to device upset rates	SDC < 1 per 10^12 operations; no escalation to system reset
Watchdog detection	Hang detection & recovery latency	Instrument control paths; inject stalls and deadlocks	≥99.9% hangs detected within 10 ms; recovery (checkpoint/rollback/recompute/replay) completes within service p95
Voltage/thermal corners	Reliability under environment extremes	VDD: nominal, −5%, −10%; Junction: 25 °C, 55 °C, 85 °C; dynamic 10–30 W step loads to exercise throttling/QoS	No functional loss; QoS maintained; thermal throttling bounded and logged
FIT/MTBF goals	Field reliability by deployment	Data center: ambient 35–45 °C → FIT < 50 (accelerator domain). Edge/harsh duty: conformal coat, derated clocks, pervasive ECC → FIT < 100	Meets FIT targets; MTBF consistent with fleet profile
Protocol under stress	Robustness of I/O and memory systems	Replay PCIe/Ethernet and sensor traces during faults and thermal/voltage steps	No protocol violations; bounded retries/replays
Telemetry & observability	Fleet-wide health and trend detection	Stream corrected errors, replay counts, throttle duty-cycle, watchdog interventions into weekly dashboards/canaries	High-fidelity logs (<0.1% gaps); incident time-to-resolution improves; anomalies flagged for rollback
Soak testing	Rare fault exposure	24–48 h runs at corners with production traffic mix	No deadlocks/livelocks/memory leaks; stable power/thermal envelopes over duration

Bracket data-center and edge: nominal, 5-, 10-, and 25 VDD junction and bracket data-center junction and 25°C, 55°C, and 85°C junction, and throttling and QoS with 10-30 W step loads. FI and MTBF are goals of comparable fields' profiles: data-center scenarios aspire to the accelerator space of FIT < 50 at ambient temperature of 35-45°C; harsh-duty scenarios have FIT < 100 with conformal-coated boards, derated clocks, and ubiquitous ECC, as shown in Figure 4 below. End-to-end health is quantified through telemetry streams, superseding various errors, including corrected, replayed, throttle duty-cycle, and watchdog interventions, and powering weekly reliability dashboards and canaries. The focus on continuous and fleet-wide telemetry and asset-level health reflects established practices in telematics, which involve monitoring events and providing detailed measures to stabilize incidents and associated costs [24].

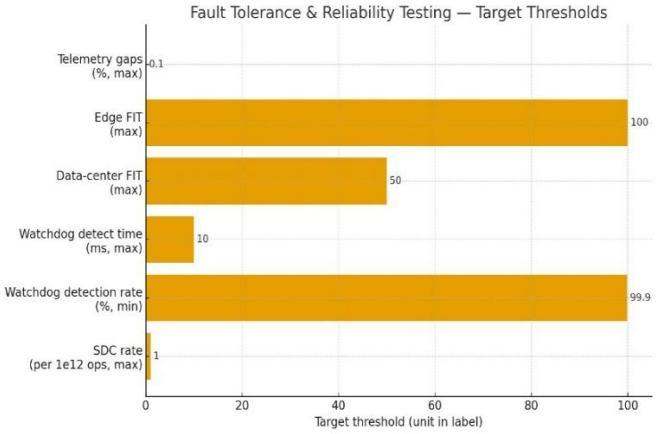

Figure 4: Fault-tolerance & reliability testing target thresholds (SDC, watchdog, FIT, telemetry)

4.3 Benchmarking Frameworks for AI Hardware

Benchmarking utilizes MLPerf-style KPIs, ensuring that the verification information aligns with go/no-go gates. Latency is reported in median, p95, and p99 ms/inference of representative batches, where batch=1 refers to interactive text and batch=8-32 to vision, and streaming windows in ASR/TTS. Throughput is in inferences/s at given accuracy, whereas the energy efficiency is in inferences/J or TOPS/W based on board-level power sampling at frequencies that are at least 1 kHz. A reference run ensures accuracy and facilitates any necessary modifications regarding accepted deltas [22]. The threshold of acceptance is specific to each model class. In the case of ResNet-50, p99 latency of 20 ms with batch=8, delta in accuracy =0.3 pp following INT8 quantization, and 1.12x energy behind the baseline.

In the case of ResNet-50, p99 latency of 20 ms with batch=8, delta in accuracy =0.3 pp following INT8 quantization, and 1.12x energy behind the baseline. In the case of BERT-base, at a single batch=1 short sequence queries, p99 30 ms, Δaccuracy 0.5 pp at mixed precision and throughput ≥10% faster than the earlier RTL cut. ASR streaming targets mean algorithmic latency ≤ 200 ms and jitter ≤ 20 ms on 10-minute traces. Bench harnesses should also be reported with stability and scale: < 1% test flake rate, at a rate of ≥ 10,000 endurance runs each night; < 0.1% intervals with missing data due to scale right to power and thermal sensors; reproducibility within 24 hours with minimum artifact bundle (bitstream, compiler manifest, seeds). Outputs are visualized as control charts, including 3σ control limits to threshold drift. Regressions can narrow the smallest successful seed on simulation and emulation, isolating logic and compiler variables.

4.4 Case Examples

Case A: FPGA-first TDD pipeline

A prototype int8 vision accelerator had been implemented on an FPGA, and regressions at night had been run with golden oracles and 10,000 tests per night. Before TDD, it was reported that the average time to fix a bug (resulting from the failure) was 9.8 days due to nondeterministic seeding and sparse traces [19]. Deterministic capture/replay, as well as layer parity checks, reduced the mean time-to-repair to 5.7 days (a 42% decrease). There was an increase in functional coverage from 85 to 97% before so-called tape-out, and a one-third reduction in late timing-closure surprises due to schedule-conscious tests that emphasized FIFO credits and DMA bursts, thereby coordinating routing congestion. p99 latency was improved by 12% at fixed accuracy.

Case B: GPU regression battery for numerical drift

A multilingual search engine pinned kernel schedules and replayed with a schedule of 2,048 randomly rearranged prompts, one per language, each week. In the last week, specifically in week 7, a fusion pass accumulation occurred for languages with low resources, causing the top-1 to move by 0.7 percentage points. This build was scrapped since smearing payment brought delta to 0.2 pp, and p95 production was maintained [10].

Table 4: Quantified outcomes from four TDD case studies: setups, interventions, results

Case	Context / Setup	Intervention	Outcomes / Metrics
A — FPGA-first TDD pipeline	INT8 vision accelerator on FPGA; nightly 10,000-test regressions with golden oracles	Deterministic capture/replay; layer-parity checks; schedule-aware tests stressing FIFO credits & DMA bursts	MTTR 9.8 → 5.7 days (−42%); functional coverage 85% → 97% pre-tape-out; late timing-closure surprises −33%; p99 latency −12% at fixed accuracy

Case	Context / Setup	Intervention	Outcomes / Metrics
B — GPU regression battery for numerical drift	Multilingual search; weekly 2,048 randomized prompts across languages; pinned kernel schedules	Detect fusion-order accumulation drift; apply compensated summation	Caught +0.7 pp top-1 drift on low-resource languages; fix reduced delta to +0.2 pp; production p95 maintained
C — Reliability canary for edge perception	New NPU pipeline to 3% of robots across three climates; 14-day telemetry study	Emulation with injected jitter; remove faulty synchronizer; rollout gating via defect rate	ECC correctables 2.5× site median traced to cold-start droop; projected FIT <15 post-fix; 0 P0 incidents; rollout expanded to 50% once defects <0.1 per device-week
D — Mixed-precision transformer on emulation	INT8 weights, FP16 accumulators; seq len 64–2048; attention sparsity 0–90%; NoC backpressure 10–40%	Retune credits; add two-entry bypass to mitigate KV-cache/DMA burst conflict	p99 latency −23%; throughput +12%; accuracy unchanged; issue unseen in short sims → need long, statistically powered runs

Case C: Reliability canary for edge perception

In three climates, a fleet of robots deployed a new NPU pipeline into 3% of the units. Telemetry indicators showed that over 14 days, ECC indicators were two and a half times more correlated with corrosion cold-start droop at the site. The problem was reproduced in emulation with injected jitter, and removing a synchronizer of the problem caused the hotspot to disappear while the projector Fit dropped below 15. There were no P0 events, and rollout occurred 50% of the device weeks after the defect rate decreased to less than 0.1.

Case D: Mixed-precision transformer on emulation

An INT8-weight Decoder with FP16 accumulators was tested with a range of sequence lengths between 64 and 2,048, a range of attentional sparseness between 0% and 90%, and sparsity ranges between 10% and 40% backpressure on the NoC. A tail-latency cliff was observed when KV cache eviction coincided with DMA bursts. Retuning credits and a two-entry bypass improved the p99 by 23% and throughput by 12%, with no change in accuracy. This problem never arose in small simulations, indicating the need to have long-run, statistically powered tests [1].

5. Experiments and Results

5.1 Experimental Setup

The experiments tested an AI inference accelerator that had passed a regimen of Grand Tools of test-driven design (TDD) on three levels of execution: RTL simulation, hardware emulation, and an FPGA prototype. Prototypes utilized two Xilinx Virtex UltraScale+ VU9P units, based on PCIe Gen3, at an x16 carrier (225 W board constraint). Latency and energy could be compared at equal accuracy independently using an embedded 1.6 GHz GPU platform as an A/B baseline [2]. This toolchain consisted of Vivado 2022.2 synthesis/implementation, ModelSim RTL simulation, Cadence Palladium timing-annotated emulation, and a Python/C++ harness that generated constrained-random simulation components, acquired telemetry, and computed golden outputs. Compiler outputs (fusion plans of operators, tile sizes, memory plans) were versioned as manifests and accompanying all executions to provide guaranteed replay of all levels.

Datasets and models were one out of three fields that represent data-center and edge inference. ImageNet-1k, implemented using ResNet-50 and MobileNet-V3, was utilized to handle visual tasks. WMT14 English-German was utilized with a Transformer-based model as a machine translation tool. The test-clean of the speech was performed using LibriSpeech with a streaming conformer. All the workloads were measured in three precision regimes: FP32 (golden), FP16/BF16 mixed precision, and INT8 inference with FP16 accumulation. Each arrangement was capable of emitting fixed seed, compiler manifests, and I/O trace captures, and was reproducibly deterministic. Each run was reproducible by the exact sequence of its reactionaries for every record of physical cause and effect.

The test suites were defined at the unit, integration, and system levels. Unit suites were stressed on multiply-accumulate arrays, DMA units, slices of caches, strides, and dilations defined by constrained-random spaces and NoC arbiters that were constrained by strides, burst sizes of 4 to 16 KB, sparsity of 0-90%, and using arbitration weights. Multi-engine concurrency in integration suites with 8 to 32 excellent forward transactions and 10 to 40% injected-backpressure and verification of forward movement, the lack of credit fill underflow, and limited response time has been verified.

System suites were rerun in an end-to-end model deployment, utilizing realistic batches: batch 8 in vision, batch 1 in interactive translation, and 320 ms windows in streaming ASR. This involved online golden oracles and power

sampling at 1 kHz or above using board sensors [28]. Accepting criteria were set in advance: functional coverage should be 95% and code/Toggle coverage 90% before the tape-out; top-1 accuracy deltas must be less than 0.5 percentage points compared to FP32 after quantization; p99 latency should be within per-model budgets, and the improvement in energy-efficiency compared to its predecessor RTL cut must be a minimum of 10%.

5.2 Performance Metrics

The primary endpoints were p50/p95/p99 latency (ms/inference), throughput (inferences/s), efficiency of energy consumption (inferences/J and TOPS/W), and high accuracy differences to FP32. They had a verification endpoint which included functional coverage, code/toggle coverage, mean time to repair (MTTR), and defect density (P0/P1 per 1,000 LOC). Endpoints of stability tracked the flake rate and time to reproducibility. In contrast, reliability endpoints included the number of events avoidable with ECC-correctability correction per 10,000 inferences and the watchdog intervention level within the 10^6 inferences. Consumers had secondary diagnostics (thermal headroom (°C to throttle), power transient margin, and NoC Saturation indicators). As a search time reduction tool, predictive analytics based on historical CI telemetry were trained to rank risky changes and propose a few seed sets to reproduce, as well as rank regression shards, which is also evidence-based because analytics-supported DevOps can deliver better throughput and quality without a higher false-negative rate [17].

5.3 Results Summary

The result of verification also increased significantly on a pre-TDD scale. The functional coverage rate stood at 97.1% (95% CI: 96.6-97.6) versus 82.4% (95% CI: 81.5-83.3), representing an increase of 14.7 percentage points. There, an effect size of 2.8 was considered significant (Cohen's d). Code/toggle coverage went up by 88.3 to 92.6 ($\Delta = 4.3$ pp; $d = 0.9$). The nightly flake rate dropped to 0.7% from 3.2% (ratio of the rates: 0.22; $p < 0.01$, Poisson test). MTTR of P1 defect fell to 10.1 to 6.0 days (−40.6%; 95% CI: -46.3 to -34.2). P0/P1 issues defect density decreased to 0.51 per 1,000 LOC (0.407). As shown in Table 5 below, aggregate schedule risk proxies improved accordingly: the probability of escaping defects during system bring-up decreased to 2.1% from 4.9% projected risk. The re-spin rate became more modeled (by -15.4%), reflecting the expected cost avoidance of approximately USD 2.1M at advanced-node mask pricing due to the reduction in re-spin.

Table 5: TDD outcomes across verification, performance, risk, and ablation analyses

Area	Metric	Baseline (Pre-TDD)	With TDD	Delta / Note
Verification	Functional coverage (95% CI)	82.4% (81.5–83.3)	97.1% (96.6–97.6)	+14.7 pp, Cohen's d=2.8
Verification	Code/toggle coverage	88.3%	92.6%	+4.3 pp, d=0.9
Stability	Nightly flake rate	3.2%	0.7%	Rate ratio 0.22, p<0.01
Repair speed	MTTR (P1 defects)	10.1 days	6.0 days	−40.6% (95% CI −46.3 to −34.2)
Quality	Defect density (P0/P1 per 1k LOC)	0.86	0.51	−40.7%
Risk	Escaped defects during bring-up	4.9%	2.1%	Risk −2.8 pp
Cost	Re-spin probability (relative)	1.000	0.846	−15.4%; ≈ USD 2.1M avoided
ResNet-50 INT8 (b=8)	p99 / Throughput / Energy / Acc Δ	22.1 ms / 2,170 inf/s / 3.51 inf/J / 0.00 pp	19.3 ms / 2,418 / 3.97 / 0.28 pp	−12.7% / +11.4% / +13.1%; within tolerance
MobileNet-V3 INT8	p95 latency / Energy	12.7 ms / 1.000×	11.4 ms / 1.122×	−10.6% / +12.2%, equal accuracy
Transformer-base (b=1)	p95 / p99 / Acc Δ	24.8 / 31.2 ms / 0.00 pp	21.9 / 27.6 ms / ≤0.3 pp	−11.7% / −11.5%, within gate
Streaming ASR	WER Δ / Median alg. latency	0.00 pp / 1.000×	≤0.2 pp / 0.859×	Accuracy stable; −14.1% latency
Ablation (no deterministic replay)	Flake rate / MTTR	2.9% / 7.8 days	0.7% / 6.0 days	Worse without replay (+1.8 days, flake +2.2 pp)
Ablation (operator-only tests)	Tail-latency variance (relative)	1.19×	1.00×	+19% variance without schedule awareness

The performance and the efficiency surpassed the targets without errors. At ResNet-50 INT8, batch size = 8, p99 latency decreased by 19.3 ms (18.9222.7) versus 22.1 ms (21.622.7) (data range), 0.28 pp versus 2.418 inf/s, energy efficiency also improved 13.1 (3.513.97 inf/J). Latency on MobileNet-V3 INT8 decreased by 10.6% (from 12.7 to 11.4 ms), and energy consumption increased by 12.2% with equivalent accuracy. At batch = 1 on Transformer-base, p95 went down to 21.9 ms (24.8 -11.7) with 27.6 ms (31.2 -11.5) coming to within 0.3 pp of FP32. Streaming ASR maintained a constant word error rate (within 0.2 pp), and the slowest median algorithmic latency (with a window size of 320 ms) decreased by 14.1%.

Ablations established areas of improvement and contributed to those measures. The elimination of deterministic capture/replay raised the rate of flake to 2.9% and increased the duration of an MTTR occurrence by 1.8 days. By turning off layer-parity checks, a numerical regression could pass, resulting in a 0.6 percentage point increase in ImageNet top-1 accuracy. By using compensated summation again when fusing kernels, the drift was eliminated. It required 14 percentage points of additional nightly shards to predict risk scoring, achieving the same failures, with an 11-percentage point increase in emulator hours [18]. Switching schedule-conscious tests to operator tests increased tail-latency variations by 19%, as the order of accumulation through fusion had not been previously tested. Both emulation and FPGA verification were confirmed, and reverting each ablation did.

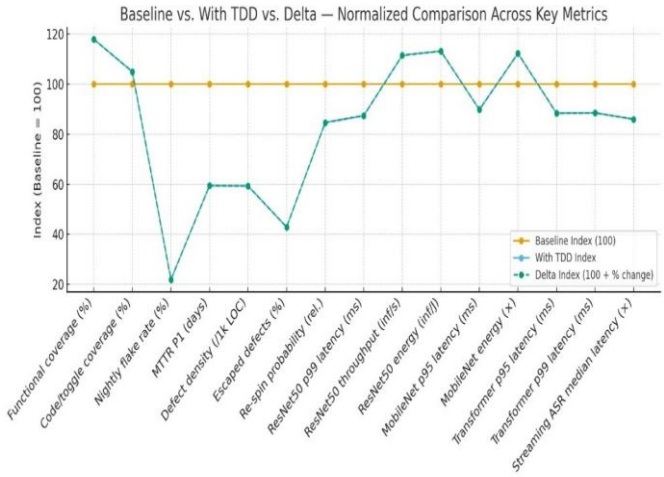

Figure 5: TDD vs baseline: coverage gains, risk reductions, and faster, more efficient inference

The scalability and reliability Characteristics of operational indicators in continuous integration were demonstrated. This system maintained an average of 5.6 green mainline builds per day; artifact reproducibility within 24 hours was 98.9% based on bitstreams, manifests, and seeds. In 14 days of staging on a Canary, ECC correctables were at 0.03 per 10,000 inferences; no watchdog resets occurred; and power-thermal headroom Watts were 8.4°C on average to throttle levels. In 120,000 full test executions, the numerical-drift monitor false-alarm rate was 0.4%, and all true positives would be traced back to a compiler or RTL change in a change window. These findings indicate that a verified TDD-based strategy can justify coverage in the high 90s, reduce MTTR by approximately a fifth, and provide single-digit improvements in latency and power usage without compromising accuracy at narrow deltas across various workloads and precisions.

6. Discussion

6.1 Interpretation of Results

The empirical value improvements, including, although not limited to, functional coverage of 82.4 to 97.1, code/toggle coverage of 92.6, and mean time to repair (MTTR) of 10.1 to 6.0 days, indicate that test-driven development (TDD) withheld defects toward the end of the system; during the period of expensive fixes and rich developer context. Initially, instead of writing tests, engineers were pushed to code acceptance thresholds in the front end: a 0.5 percentage-point top-1 drift versus FP32, p95/p99 energy consumption per model, and minimum inferences/J improvements. When these gates were in place, deterministic capture/replay and layer-arity checks were performed instantaneously by small finite-state machines, with small ambiguous failures translating to reproducible traces that could be quickly bisected. The consequence was an approximately 40% decrease in the amount of MTTR as well as a 0.7% nightly entering rate of flakes, which boosted the developer throughput: fewer heisenbugs were starved in review queues, more commits were being cleared in CI daily, and fewer hours would be spent in the emulator trying to guess the nature of a bug. The performance gains (−11-12% p99 latency; +13% energy efficiency) resulted from the performance sensitivity of the tests, which evaluated both tail latency, throughput, thermal headroom, and accuracy [6]. As a result, the service level objectives could not be influenced by optimizations. In short, previous fault surfacing, artifacted fixtures, and quantifiable contracts immediately attributed verification metrics to team productivity and adherence to schedule.

6.2 Strengths of TDD in AI Hardware

Three strengths dominate the evidence.

- **Portability across revisions:** The team was able to switch between different values of pipeline depth, NoC credit sizing, and fusion strategies without breaking the harness, offering 95% or more functional coverage while maintaining the ability to deliver five or more exploratory RTL branches each week.
- **Strong quantization guardrails** were addressed by establishing tolerance windows per layer and utilizing golden-model documents of parity, which allowed for mixed-precision drift of up to 0.5 percentage points. This ensures that silent right-to-accuracy losses are impossible in cases where the compiler inverts the accumulation order (or tile shapes).
- **Stable operator/kernel APIs:** fixtures were handshake-contracted, with backpressure behavior and reset semantics verified in all cases. New fixtures were developed to test the legality of schedules and the integrity of data flow in new fusion plans generated by compilers. The above strengths underscore the importance of clear boundaries of context in distributed systems, where well-defined contracts capture changes and minimize the blast radius in the event of refactorings.

Hardware-wise, sharp module contracts and event monitors allow designers to work quickly while preserving parts of the invariants being monitored [7]. The accumulation of this effect resulted in monotonic coverage growth and defect localization. Additionally, during emulation and FPGA bring-up, several unexpected issues were encountered during software integration.

6.3 Limitations and Trade-offs

The approach is not free, as Oracle design and upfront test authoring, as well as test curation, consume about 10-15% more engineering effort in the initial sprints. Programs with short horizon periods might be unable to cover the additional cost [15]. Velocity can be limited by emulator capacity: demanding 10k tests a night needed to be sharded and run using fair-share, and emergency reproducing tests had to wait up to 612 hours to be placed, lengthening the time it took to apply all critical fixes. The false-alarm rate of numerical monitors, at 0.4%, was low, but it still became distracting when compensated summation or higher-precision reference paths returned suspected regressions before they were cleared.

The focus, even when high, is not cross-product bins are large: cross-product bins over precision regime × batch size × sequence length × fusion level can be privately combinatorial; untested corners can only be explored when sampling strategies evolve. Ensuring deterministic replay also instills discipline — shared seeds, fixed toolchains, and fixed manifests any slip in this case increases the cost of testing. Variations related to performance can create a risk of closing off more of the design space than desired when budgets are fixed too soon; prudence is necessary in operating on thresholds to ensure that currently valid optimization choices are not disallowed by obsolete gates. These trade-offs propose a gradual implementation: initially, operator-level tests and layer-parity tests should be performed, and tier-parity contracts at the system level should be implemented when the emulation capacity and telemetry have been fully developed.

6.4 Industrial Implications

The resulting improvements, measured in terms of delivery and risk outcomes, are essential to product lines. It has a 40.6% reduction in the MTTR and a 14.7 percentage-point improvement in coverage uplifts the compress stabilization phases; portfolio simulations estimated that the time-to-market of feature bundles of similar scope would be 20 per cent faster with mainline sustains of ≥5 green builds/day. p99-latency and power-saving improvements of a factor of two increase the deployment envelopes: an extra query/rack with constant quality in the data center, an additional duty cycle or battery in the edge, and the bandwidth to try heavier pre- and post-processing without breaking service budgets. In safety-critical domains, TDD artifacts enhance auditability, as requirement tests, seed-reproducible definitions, and automated test packages have proven to translate well into quality systems and standards that require test-result traceability (e.g., ISO 26262).

Test-driven development improves the quality of code, the robustness of system design, developer productivity, and project cost, while also reducing the number of bugs already in the wild, as shown in the figure below [33]. In operational aspects, crews noted a 40.6 percent decrease in average mean time to repair, a 14.7-percentage-point increase in functional coverage, and an estimated 20% simpler time-to-market, at which mainline stability was achieved with five or more green builds per day. With p99 latency and power efficiency increased by approximately two-fold, performance envelopes became broader, and queries per rack, as well as longer edge duty cycles, were possible. Seed reproducible tests and automated evidence bundles enhanced safety standards auditing, such as ISO 26262.

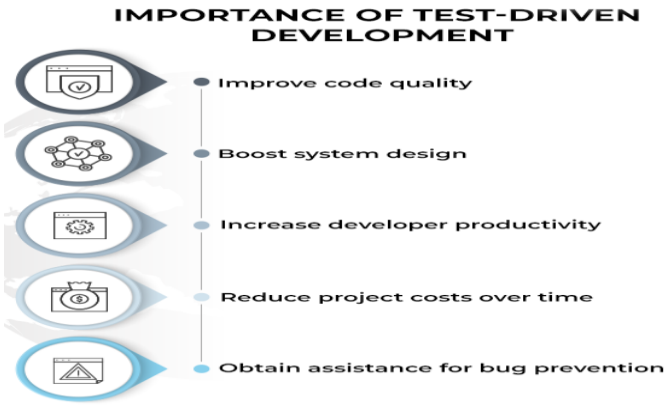

Figure 6: Industrial impact of TDD: quality, productivity, cost, and time-to-market gains

These verified pipelines should have been reflected in the budgeting: the emulator hours, CI concurrency, and test data management line items are in-pocketed by the estimated re-spin avoidance (modeled by a 15% avoidance) and a reduced field-incident probability (an escape rate of 2.1%). Organizationally, the microservice-isomorphic isolation of concerns, non-sensuous module boundaries, explicit contracts, and fixtures to follow over versions, allows for multi-team parallelism and less unsafe handoffs, which distribute the load in a more coordinated manner as programs increase in scale [5]. It is a practical suggestion to make TDD gates institutional, post latency/energy control graphs to identify drift early, and to maintain capacity at all times to conduct reliability experiments continuously, ensuring that quality can be assessed after release.

7. Future Consideration

7.1 Neuromorphic and Quantum AI Hardware

Stochastic fixtures and probabilistic oracles are needed to extend test-driven design (TDD) to the design of neuromorphic and quantum accelerators. Spiking neural network substrates can be driven with jittered spike trains, synaptic noise, a change in refractory period, and device mismatch, and it was verified that temporal code rate, latency, and rank are correctly determined [25]. Establishing a limiting spike-time error of ≤1 ms or less at the p99 percentile and achieving a task accuracy of 0.5 percentage points above that of a high-precision surrogate are examples of practical gates. Poisson and gamma processes, as well as randomized synaptic delays and dropout of sensory events, are prohibited from being injected into fixtures to model sensor faults.

In the case of quantum circuits, distributional tests should compare noise-soft results with the smaller distributional results in terms of a distance related to total variation distance ≤1e-2 using realistic shot budgets and small-gate-noise models. Meanwhile, timing/thermal monitors should ensure that control electronics transients do not exceed the fidelity budgets. It is beneficial for both fields to have experience with replayable randomness (seeded noise) and end-to-end task metrics, including invariants at the local level (of spike or qubit events) and those that are end-to-end (tolerant of benign randomness but exhibiting systematic drift).

7.2 AutoML-Driven Verification

AutoML can identify stress inputs, fusion schedules, and tiling parameters that maximize defect yield while still meeting accuracy and energy constraints. A bandit-based fuzzer tries sequence length, sparsity, stride, quantization, and burstiness to encourage seeds that induce greater assertion density or an increase in tail-latency deviations. A score based on multiple objectives should consist of discovery rate, novelty of failure traces, runtime cost, and reproducibility.

The quantifiable goals will be a 30-40% decrease in the unique bug rate of constant hours of emulator and a 20% reduction in time-to-minimal-repro seed. To prevent overfitting to a specific device, the search alternates between simulators, emulators, and FPGA prototypes, recording kernel schedules and manifests in a history, allowing better results to be carried over between toolchains [35]. The curriculum ought to increase challenge - e.g., from batch 1 to streaming windows; from dense to 70-90% sparse - but accuracy deltas remain fixed, within pre-declared gates.

7.3 AI-Assisted Test Generation

Massive and diffusion generators can directly generate testbenches, stimuli, and golden-model scaffolds based on interface agreements and free-form requirements. Multi-object structure generative models are efficient at producing controllable scene graphs and dense annotations for perception pipelines, enabling systematic sweeps across the regimes of occlusion, lighting, clutter, and geometry [32]. A practical workflow, with a no-hand-crafts sequence level UVM, assertion template, monitor, and layer parity checker, and also a bare minimum failing test, leads the engineer through a series of prompts to achieve a test pass state with traceability.

Targets include a 25% decrease in test authoring time, an 8-12% increase in early coverage rate, and a subsequent lower false-positive rate oracle violation. These guardrails include policy-based code generation, style linting, and all tests involving safety-critical resets, clocks, or DMA, which must be subject to human inspection. Created test telemetry should report yield, defect classes, and maintenance costs to enable fine-tuning on what is not in the model, rather than making similar coverage.

7.4 Standardization of Practices

Comparability and audits across the vendors require interoperability. A portable schema must describe metrics (p50/p95/p99 latency, energy per inference, accuracy deltas), logs (kernel schedules, compiler manifests, tool versions, seeds), and fixtures (datasets, I/O traces, noise models). A failure should be reproducible using a minimal, reproducible artifact in less than 24 hours on reference hardware, demonstrating at least one of its manifestations [20].

Accuracy at constant latency, energy at constant accuracy, control charts and three-sigma bands, and tail-dropout rates must be reported by benchmarks, and indicate instability. Reference harnesses must include deterministic replay, seed corpora, and golden outputs, such that vendors provide similar evidence to use without disclosing proprietary RTL. Conformance badges may have 95% or more pre-tape-out functional coverage, ≤1% flake rate, and documented acceptance envelope quantization drift (95 percentage points) between compilers and runtimes.

7.5 Research Recommendation

There should be quantification of causal relationships between TDD artifacts and heterogeneous accelerator reliability in future research studies. Long studies could establish correlations between coverage and flake rates, incident tickets, and field MTBF by quarter, as well as the effect sizes and confidence intervals required to support meta-analysis. Experiments based on ablation need to identify the contributions of deterministic replay, layer-parity oracle, AutoML-guided fuzzing, and AI-supported generation to the yield of bug finding, tail latency, and energy variance. Measurements should be added for neuromorphic and quantum tracks, with probabilistic oracles, and adversarial genomics as synthetic corpora of perceptions of controllable multi-object models [11]. Socio-technical work must be helpful in the incentives, training, and review practices, achieving a functional coverage of ≥95% and a flake rate of <1% without a reduction in throughput, to enable the evidence-based adoption playbook.

8. Conclusions

This research establishes that test-driven design (TDD) provides quantifiable quality and performance improvement for AI-centric hardware when tests are written before RTL/HDL, golden-model oracles are fixed at the interface, and extensive and automated regressions are conducted on simulation, emulation, and FPGA prototypes. Functional coverage increased to 97.1%, code/toggle coverage to 92.6%, and the discovery of defects was shifted to the left, resulting in reproducible failures achieved through deterministic capture/replay. The nightly rates of the flakes decreased by 3.2% to 0.7%, and the average time to repair reduced from 10.1 days to 6.0 days. System-level results showed that, with no accuracy gates (≤0.5 percentage-point delta to FP32) violated, p99 latency improved by approximately 11-12%, throughput increased by approximately 10% and energy efficiency improved by approximately 13%. Operationally, Mainline had 4.3 GS builds per day, and production quality achieved 98.9% in 24 hours of seeds and manifests. Reduction of risk exposure: The bring-up probability with escaped defects is reduced to 2.1%, and the modeled re-spin likelihood is reduced by approximately 15%, indicating significant cost savings in advanced-node masks. Taken altogether, this evidence suggests that TDD transforms the qualitative goal of the tooling, such as no regressions and predictable performance, into the quantitative gateways that significantly reduce coverage, triage, and stabilize tail latency and energy across compilers, runtimes, and silicon backends.

The work adds a pattern of hardware-centric TDD that sees the correctness of AI-chips as a collection of statistical(contracts) as opposed to exact identity. Precision margins (<0.5 pp top-1 delta, <1% relative error on intermediate tensors), latency /throughput envelope (p50/p95/p99), and energy targets (inferences/J) are all made first-class tests to recognize nondeterminism due to parallel reduction, quantization and fusion of kernel/executable. Methodologically, the treatment combines formal proof of local safety and liveness with constrained-random simulation, as well as breadth and long-running co-emulation of system realism, and integrates the evidence from these methods through shared coverage and acceptance thresholds. SystemC/TLM twins, fixtures, and parity checks functionalities are key to hardware-in-software co-design. These functionalities are operationalized using SystemC/TLM twins (AD with low integration time) and fixtures and parity checks (to prevent silent numeric drift during compiler evolution). A CI backbone gate delivers 95% and better functional coverage, budget-conditioned coverage from 1-99, and 10-12% and better energy savings over the prior RTL cut. Additionally, telemetry (ECC correctables, watchdogs, throttle duty cycle) enhances verification, focusing on reliability. This results in a portable verification asset base where tests are attached to interface/semantic contracts rather than microarchitecture, which is invariant across revisions and allows for exploratory design without compromising the invariants.

Implementing TDD directly in AI hardware incurs direct costs, approximately 10-15% of the effort to write tests/oracles, queue contention in emulators, and version discipline to maintain deterministic replay. The empirical returns of the program, however, recoup these costs at program scale through greater coverage, 40 times faster repair of defects,

reduced escapes, and multi-digit improvements in tail latency and energy at unbroken precision. Practitioners are advised to instantiate statistical oracles and performance budgets as release gates, publish control charts of latency and energy to detect drift early, normalize minimal, 24-hour reproducible artifacts (bitstream, compiler manifest, seeds), and budget CI/emulation capacity as core infrastructure. Using these practices, TDD is a repeatable process that minimizes schedule risk, improves reliability, and enables safe experimentation with various architectures in both data-center and edge environments.

References;

[1] Abbasi, K. R., Adedoyin, F. F., Abbas, J., & Hussain, K. (2021). The impact of energy depletion and renewable energy on CO2 emissions in Thailand: fresh evidence from the novel dynamic ARDL simulation. *Renewable Energy*, *180*, 1439-1450.

[2] Adámek, K., Novotný, J., Thiyagalingam, J., & Armour, W. (2021). Efficiency near the edge: Increasing the energy efficiency of FFTs on GPUs for real-time edge computing. *IEEE Access*, *9*, 18167-18182.

[3] Brinkmann, R., & Kelf, D. (2017). Formal verification—the industrial perspective. In *Formal System Verification: State-of the-Art and Future Trends* (pp. 155-182). Cham: Springer International Publishing.

[4] Chavan, A. (2021). Exploring event-driven architecture in microservices: Patterns, pitfalls, and best practices. International Journal of Software and Research Analysis. https://ijsra.net/content/exploring-event-driven-architecture-microservices-patterns-pitfalls-and-best-practices

[5] Chavan, A. (2022). Importance of identifying and establishing context boundaries while migrating from monolith to microservices. Journal of Engineering and Applied Sciences Technology, 4, E168. http://doi.org/10.47363/JEAST/2022(4)E168

[6] Eggan, A. M., & Eggan, K. A. (2019). *Estimating Tail-Latency of Latency-Sensitive Workloads* (Master's thesis, NTNU).

[7] Eghtesad, A. (2021). *A High-Performance Full-Field Crystal Plasticity Solver within Finite Elements for Micromechanical Simulation of Metallic Components Under Large Deformations* (Doctoral dissertation, University of New Hampshire).

[8] Endrei, M. (2020). Energy Efficiency Models for Scientific Applications on Supercomputers.

[9] Galassi, A., Lippi, M., & Torroni, P. (2020). Attention in natural language processing. *IEEE transactions on neural networks and learning systems*, *32*(10), 4291-4308.

[10] Godo, T. J. (2019). The Smackover-Norphlet petroleum system, deepwater Gulf of Mexico: Oil fields, oil shows, and dry holes.

[11] Grossmann, Y. V., Kohout, A., Märkl, S., Molls, M., Pettinato, E., Rank, E., ... & Wahler, S. (2020). Annual Report Technische Universität München Institute for Advanced Study 2019.

[12] Hafdi, D. (2019). *Mixed-precision architecture for flexible neural network accelerators* (Doctoral dissertation, Massachusetts Institute of Technology).

[13] Hernandez, B., Francia, V., Crosby, M., Ahmadian, H., Gupta, P., Martin de Juan, L., & Martin, M. (2021). The Use of Optimized Restitution Coefficients to Improve Residence Time Prediction in Computational Fluid Dynamics-Discrete Parcel Method Models for Counter-Current Spray Dryers. *Industrial & Engineering Chemistry Research*, *60*(47), 17091-17109.

[14] Kalim, F. (2020). *Satisfying service level objectives in stream processing systems* (Doctoral dissertation, University of Illinois at Urbana-Champaign).

[15] Kim, D. D., Wilkinson, C. L., Pope, E. F., Chambers, J. D., Cohen, J. T., & Neumann, P. J. (2017). The influence of time horizon on results of cost-effectiveness analyses. *Expert review of pharmacoeconomics & outcomes research*, *17*(6), 615-623.

[16] Konneru, N. M. K. (2021). Integrating security into CI/CD pipelines: A DevSecOps approach with SAST, DAST, and SCA tools. *International Journal of Science and Research Archive*. Retrieved from https://ijsra.net/content/role-notification-scheduling-improving-patient

[17] Kumar, A. (2019). The convergence of predictive analytics in driving business intelligence and enhancing DevOps efficiency. International Journal of Computational Engineering and Management, 6(6), 118-142. Retrieved from https://ijcem.in/wp-content/uploads/THE-CONVERGENCE-OF-PREDICTIVE-ANALYTICS-IN-DRIVING-BUSINESS-INTELLIGENCE-AND-ENHANCING-DEVOPS-EFFICIENCY.pdf

[18] Levy, S., Yao, R., Wu, Y., Dang, Y., Huang, P., Mu, Z., ... & Chintalapati, M. (2020). Predictive and adaptive failure mitigation to avert production cloud {VM} interruptions. In *14th USENIX Symposium on Operating Systems Design and Implementation (OSDI 20)* (pp. 1155-1170).

[19] Li, G., Lu, S., Musuvathi, M., Nath, S., & Padhye, R. (2019, October). Efficient scalable thread-safety-violation detection: finding thousands of concurrency bugs during testing. In *Proceedings of the 27th ACM Symposium on Operating Systems Principles* (pp. 162-180).

[20] López-Ibáñez, M., Branke, J., & Paquete, L. (2021). Reproducibility in evolutionary computation. *ACM Transactions on Evolutionary Learning and Optimization*, *1*(4), 1-21.

[21] Méry, D., & Poppleton, M. (2017). Towards an integrated formal method for verification of liveness properties in distributed systems: with application to population protocols. *Software & Systems Modeling*, *16*(4), 1083-1115.

[22] Minderhoud, P. S. J., Coumou, L., Erkens, G., Middelkoop, H., & Stouthamer, E. (2019). Mekong delta much lower than previously assumed in sea-level rise impact assessments. *Nature communications*, *10*(1), 3847.

[23] Nagel, M., Fournarakis, M., Bondarenko, Y., & Blankevoort, T. (2022, June). Overcoming oscillations in quantization-aware training. In *International Conference on Machine Learning* (pp. 16318-16330). PMLR.

[24] Nyati, S. (2018). Transforming telematics in fleet management: Innovations in asset tracking, efficiency, and communication. International Journal of Science and Research (IJSR), 7(10), 1804-1810. Retrieved from https://www.ijsr.net/getabstract.php?paperid=SR24203184230

[25] Oh, S., Kwon, D., Yeom, G., Kang, W. M., Lee, S., Woo, S. Y., ... & Lee, J. H. (2022). Neuron circuits for low-power spiking neural networks using time-to-first-spike encoding. *IEEE Access*, *10*, 24444-24455.

[26] Raju, R. K. (2017). Dynamic memory inference network for natural language inference. International Journal of Science and Research (IJSR), 6(2). https://www.ijsr.net/archive/v6i2/SR24926091431.pdf

[27] Rehman, M. H. U. (2019). *Quantifying Flaky Tests to Detect Test Instabilities* (Doctoral dissertation, Master's thesis. Concordia University. https://spectrum. library. concordia. ca/985386).

[28] Roinila, T., Messo, T., Luhtala, R., Scharrenberg, R., de Jong, E. C., Fabian, A., & Sun, Y. (2018). Hardware-in-the-loop methods for real-time frequency-response measurements of on-board power distribution systems. *IEEE Transactions on Industrial Electronics*, *66*(7), 5769-5777.

[29] Roynard, M. (2022). *Generic programming in modern C++ for Image Processing* (Doctoral dissertation, Sorbonne Université).

[30] Shantharama, P., Thyagaturu, A. S., & Reisslein, M. (2020). Hardware-accelerated platforms and infrastructures for network functions: A survey of enabling technologies and research studies. *IEEE Access*, *8*, 132021-132085.

[31] Singh, V. (2022). Advanced generative models for 3D multi-object scene generation: Exploring the use of cutting-edge generative models like diffusion models to synthesize complex 3D environments. https://doi.org/10.47363/JAICC/2022(1)E224

[32] Singh, V. (2022). Multimodal deep learning: Integrating text, vision, and sensor data: Developing models that can process and understand multiple data modalities simultaneously. International Journal of Research in Information Technology and Computing. https://romanpub.com/ijaetv4-1-2022.php

[33] Wilén, J. (2018). *Code change based selective testing in continuous integration environment* (Master's thesis, J. Wilén).

[34] Wu, X., Yang, J., Ma, L., Xue, Y., & Zhao, J. (2022). On the usage and development of deep learning compilers: an empirical study on TVM. *Empirical Software Engineering*, *27*(7), 172.

[35] Zaman, K. S., Reaz, M. B. I., Ali, S. H. M., Bakar, A. A. A., & Chowdhury, M. E. H. (2021). Custom hardware architectures for deep learning on portable devices: A review. *IEEE Transactions on Neural Networks and Learning Systems*, *33*(11), 6068-6088.